



# Human Single-chain Variable Fragments Neutralize *Pseudomonas aeruginosa* Quorum Sensing Molecule, 3O-C12-HSL, and Prevent Cells From the HSL-mediated Apoptosis

Sirijan Santajit<sup>1</sup>, Watee Seesuy<sup>2</sup>, Kodchakorn Mahasongkram<sup>2</sup>, Nitat Sookrung<sup>2,3</sup>, Pornpan Pumirat<sup>1</sup>, Sumate Ampawong<sup>4</sup>, Onrapak Reamtong<sup>5</sup>, Manas Chongsa-Nguan<sup>6</sup>, Wanpen Chaicumpa<sup>2</sup> and Nitaya Indrawattana<sup>1\*</sup>

## OPEN ACCESS

### Edited by:

Marco Rinaldo Oggioni,  
University of Leicester,  
United Kingdom

### Reviewed by:

Song Lin Chua,  
The Hong Kong Polytechnic  
University, Hong Kong  
Rodolfo Garcia-Contreras,  
National Autonomous University  
of Mexico, Mexico

### \*Correspondence:

Nitaya Indrawattana  
nitaya.ind@mahidol.ac.th

### Specialty section:

This article was submitted to  
Antimicrobials, Resistance  
and Chemotherapy,  
a section of the journal  
Frontiers in Microbiology

Received: 18 December 2019

Accepted: 07 May 2020

Published: 24 June 2020

### Citation:

Santajit S, Seesuy W, Mahasongkram K, Sookrung N, Pumirat P, Ampawong S, Reamtong O, Chongsa-Nguan M, Chaicumpa W and Indrawattana N (2020) Human Single-chain Variable Fragments Neutralize *Pseudomonas aeruginosa* Quorum Sensing Molecule, 3O-C12-HSL, and Prevent Cells From the HSL-mediated Apoptosis. *Front. Microbiol.* 11:1172. doi: 10.3389/fmicb.2020.01172

<sup>1</sup> Department of Microbiology and Immunology, Faculty of Tropical Medicine, Mahidol University, Bangkok, Thailand, <sup>2</sup> Center of Research Excellence on Therapeutic Proteins and Antibody Engineering, Department of Parasitology, Faculty of Medicine Siriraj Hospital, Mahidol University, Bangkok, Thailand, <sup>3</sup> Biomedical Research Unit, Department of Research, Faculty of Medicine Siriraj Hospital, Mahidol University, Bangkok, Thailand, <sup>4</sup> Department of Tropical Pathology, Faculty of Tropical Medicine, Mahidol University, Bangkok, Thailand, <sup>5</sup> Department of Tropical Molecular Biology and Genetics, Faculty of Tropical Medicine, Mahidol University, Bangkok, Thailand, <sup>6</sup> Faculty of Public Health and Environment, Pathumthani University, Pathum Thani, Thailand

The quorum sensing (QS) signaling molecule, *N*-(3-oxododecanoyl)-*L*-homoserine lactone (3O-C12-HSL), contributes to the pathogenesis of *Pseudomonas aeruginosa* by regulating expression of the bacterial virulence factors that cause intense inflammation and toxicity in the infected host. As such, the QS molecule is an attractive therapeutic target for direct-acting inhibitors. Several substances, both synthetic and naturally derived products, have shown effectiveness against detrimental 3O-C12-HSL activity. Unfortunately, these compounds are relatively toxic to mammalian cells, which limits their clinical application. In this study, fully human single-chain variable fragments (HuscFvs) that bind to *P. aeruginosa* haptenic 3O-C12-HSL were generated based on the principle of antibody polyspecificity and molecular mimicry of antigenic molecules. The HuscFvs neutralized 3O-C12-HSL activity and prevented mammalian cells from the HSL-mediated apoptosis, as observed by Annexin V/PI staining assay, sub-G1 arrest population investigation, transmission electron microscopy for ultrastructural morphology of mitochondria, and confocal microscopy for nuclear condensation and DNA fragmentation. Computerized homology modeling and intermolecular docking predicted that the effective HuscFvs interacted with several regions of the bacterially derived ligand that possibly conferred neutralizing activity. The effective HuscFvs should be tested further *in vitro* on *P. aeruginosa* phenotypes as well as *in vivo* as a sole or adjunctive therapeutic agent against *P. aeruginosa* infections, especially in antibiotic-resistant cases.

**Keywords:** *Pseudomonas aeruginosa*, quorum sensing, *N*-3-oxo-dodecanoyl-*L*-homoserine lactone (3O-C12-HSL), apoptosis, human scFv

## INTRODUCTION

*Pseudomonas aeruginosa*, a versatile and ubiquitous Gram-negative bacterium, is an opportunistic microorganism that frequently causes severe nosocomial infections, particularly among immunocompromised patients and those suffering from cystic fibrosis, burns, HIV infection, and cancer (Tang et al., 1996; Sadikot et al., 2005; Silva Filho et al., 2013; Malhotra et al., 2019; Waters and Goldberg, 2019). The pathogenicity of *P. aeruginosa* is attributable mainly, if not solely, to the regulons of two complete *N*-acyl homoserine lactone (AHL)-dependent quorum sensing (QS) systems, called LasI/R and RhlI/R (Preston et al., 1997; Venturi, 2006). The two QS systems act in a hierarchical manner, i.e., the LasI/R system controls the activity of the rhlI/R circuit (Pearson et al., 1994, 1995). During bacterial infection, the LasI and RhlI synthases produce *N*-(3-oxododecanoyl)-*L*-homoserine lactone (3O-C12-HSL) and *N*-butanoyl-*L*-homoserine lactone (C4-HSL), respectively. The QS molecules then interact with their cognate LasR and RhlR, causing transcription of hundreds of target genes, including those coding for virulence factors such as lectins, elastases, proteases, exotoxin A, pyocyanin, and surface-active rhamnolipids important in the late stages of biofilm development, as well as genes involved in antibiotic resistance (Wagner et al., 2003; Venturi, 2006; Rutherford and Bassler, 2012; Moradali et al., 2017).

*N*-(3-Oxododecanoyl)-*L*-homoserine lactone (3O-C12-HSL) is the prominent autoinducer of the *P. aeruginosa* QS system (Duan and Surette, 2007; Rasamiravaka and El Jaziri, 2016). 3O-C12-HSL is a small, fatty acid-like, membrane-permeant signaling molecule that comprises a hydrophilic homoserine lactone ring linked to the hydrophobic 12-carbon-atom-long acyl side chain via an amide bond (Eberhard et al., 1981; Pearson et al., 1995; Ritchie et al., 2007; O'Connor et al., 2015). The roles of 3O-C12-HSL in pathogenesis and modulation of the host immune responses have been reviewed (Liu et al., 2015). Owing to its lipophilicity, the 3O-C12-HSL can traverse the mammalian cell membrane (Ritchie et al., 2007), causing mitochondrial damage and dysfunction, which subsequently activates the caspase pathway leading to apoptosis of several cell types, including macrophages, neutrophils, T lymphocytes, human vascular endothelial cells, murine fibroblasts, airway epithelial cells, goblet cells, and breast carcinoma cells (Tateda et al., 2003; Li et al., 2004; Shiner et al., 2006; Jacobi et al., 2009; Schwarzer et al., 2012; Tao et al., 2016, 2018). *P. aeruginosa* QS signaling molecules also modulate host immune responses by down-regulating the expression of co-stimulatory molecules on dendritic cells (DCs), leading to inhibition of DC maturation and their ability to activate effector T-cell responses (Boontham et al., 2008). Because the 3O-C12-HSL plays an important role in the virulence and pathogenesis of *P. aeruginosa* and host immunity suppression, it is an attractive target for novel therapeutics for *P. aeruginosa* infection. Substances that interfere with *P. aeruginosa* 3O-C12-HSL activity should mitigate bacterial-associated disease severity, although blocking the QS system alone does not necessarily abrogate all *P. aeruginosa* virulence factors, such as T3SS (Bleves et al., 2005; López-Jácome et al.,

2019; Soto-Aceves et al., 2019). A therapeutic approach based on QS interference and/or attenuation of QS signals should result in greater sensitivity of the *P. aeruginosa* to stresses, such as antimicrobial drugs (Rasmussen and Givskov, 2006; Defoirdt et al., 2010; Maeda et al., 2012; Kalia et al., 2014; Krzyżek, 2019).

Recently, a murine monoclonal antibody (mAb), RS2-1G9, against a lactam mimetic of 3O-C12-HSL has been shown to prevent apoptosis through p38 mitogen-activated protein kinase activation and protected murine bone marrow-derived macrophages from the cytotoxic effects of the QS molecule (Kaufmann et al., 2006, 2008). The RS2-1G9 paratope was shown to enclose the polar lactam moiety of the 3O-C12-HSL molecule in the co-crystal structure of the Fab fragment of the RS2-1G9 mAb and the target 3O-C12-HSL completely (Debler et al., 2007). Active immunization of mice with 3O-C12-HSL-protein conjugate protected immunized mice from lethal *P. aeruginosa* infection (Miyairi et al., 2006). Antibody-based therapy directed to the QS molecule should not only block bacterial virulence, but also rescue the host immunity that had been modulated/suppressed by the QS system (Kaufmann et al., 2008; Palliyil and Broadbent, 2009). The present study generated engineered, fully human, single-chain antibody variable fragments (HuscFvs) that neutralize 3O-C12-HSL bioactivity. The HuscFvs should be tested, step-by-step, toward clinical application as a sole or adjunct therapy for the currently failing antibiotic treatment of patients with *P. aeruginosa* infection.

## MATERIALS AND METHODS

### *P. aeruginosa*

#### *N*-(3-Oxododecanoyl)-*L*-Homoserine Lactone (3O-C12-HSL)

The QS molecule was synthesized commercially (Cayman Chemical, Ann Arbor, MI, United States) under the IUPAC name: 3-oxo-*N*-[(3*S*)-2-oxooxolan-3-yl]-dodecanamide. 3O-C12-HSL was stored in 100% dimethyl-sulfoxide (DMSO) and diluted with phosphate-buffered saline, pH 7.4 (PBS), to the desired concentration for use.

#### Preparation of HuscFv to *P. aeruginosa* 3O-C12-HSL

The human single-chain variable fragments (HuscFvs) to the 3O-C12-HSL were generated based on the principles of the polyspecific property of an antibody, i.e., one antibody can bind different antigens by paratope adaptation to accommodate distinct antigens, such as through differential engagements of the complementarity determining regions (CDRs), and the molecular mimicry of the antigens (different antigens can share surface topologies in terms of shape or chemical nature) (Tapryal et al., 2013). In this study, HB2151 *Escherichia coli* clones carrying phagemids with inserted HuscFv genes (*huscfv*s) were previously selected from a HuscFv phage display library (Kulkeaw et al., 2009) using *Pseudomonas* exotoxin A (ETA) as antigen in the phage-biopanning process (Santajit et al., 2019). Genes coding for

HuscFvs of individual *E. coli* clones were sequenced and deduced, and the canonical CDRs and framework regions (FRs) of both VH and VL domains were determined based on the numbering scheme of Chotia and Kobat (Abhinandan and Martin, 2008).

Three dimensional (3D) models of the selected HuscFvs were generated by subjecting their deduced amino acid sequences to the I-TASSER online server (Yang et al., 2015). The HuscFvs-3D models from the I-TASSER were further refined to improve local geometric and physical quality using ModRefiner (Xu and Zhang, 2011). The quality of the generated homology models of HuscFvs was then evaluated using the PROCHECK server to provide Ramachandran plots (Laskowski et al., 1993). Thereafter, the 3D structures of the individual HuscFvs were superimposed with the 3D structure of the mAb RS2-1G9 F(ab')<sub>2</sub> (PDB ID: 2NTF) (previously shown to neutralize 3O-C12-HSL pathogenic activity; hence, the mAb has been designated as a “quorum quenching antibody”) (Kaufmann et al., 2006, 2008) using the CLICK server, i.e., the topology-independent tool comparing 3D structures without a scoring function measuring structural similarity (Nguyen et al., 2011). The HuscFvs showing top-scored topological similarity with the RS2-1G9 antigen-binding site were selected. The 3D structure of 3O-C12-HSL was retrieved from the PubChem database, a resource of chemical molecules and their bioactivities (PubChem CID: 3246941) (Kim et al., 2015). The modeled-3O-C12-HSL F(ab')<sub>2</sub> was docked with the 3D model of each HuscFv receptor binding pocket using Autodock Vina software (Trott and Olson, 2010; Forli et al., 2016). The conformation of each HuscFv-ligand complex with the lowest binding free energy ( $\Delta G$ ) at the best docking position was selected for interaction analysis and visualization through the Discovery studio visualizer 3.5 program.

## Large-Scale Production of HuscFvs

The *E. coli* clones carrying phagemids containing the DNA coding for the selected HuscFvs were subjected to sub-cloning for large scale HuscFv production. The *huscFvs* were PCR-amplified from the *huscFv*-pCANTAB5E phagemids of HB2151 *E. coli* clones using a Phusion High-Fidelity DNA polymerase (Thermo Fisher Scientific, Carlsbad, CA, United States). The PCR specific primers were forward-*huscFv*-LIC: 5'-GGTTGGGAATTGCAAGCGGC CCAGCCGGCC-3' and reverse-*E-tag*-LIC: 5'-GGAGATGGGA AGTCATTAACGGGTTCCAGCGGATCC-3'. The *huscFv* inserts were designed to consist of a HuscFv-coding sequence linked to specific sequences for ligation independent cloning (LIC) protocol (Thermo Fisher Scientific). The amplified *huscFv-E-tag* DNAs were cloned separately into the pLATE52 vector (Thermo Fisher Scientific). Recombinant pLATE52-*huscFv* plasmids were transformed into JM109 *E. coli* by the heat-shock method. After PCR screening and DNA sequencing, the recombinant plasmids were introduced into an expression host, NiCo21(DE3) *E. coli* (New England Biolabs, St. Albans, Herts, United Kingdom), and the transformed bacteria were grown at 37°C for 16 h on LB agar containing 100 µg/ml of ampicillin. A single colony of each transformed clone was cultured in LB broth containing 100 µg/ml ampicillin with

shaking (250 rpm) at 37°C for 16 h. The overnight cultures (12.5 ml) were separately inoculated into the fresh LB medium (250 ml) containing ampicillin and grown at 37°C until an OD<sub>600 nm</sub> reached ~0.6–0.8. Recombinant HuscFv expression was induced by adding isopropyl-β-D-1-thiogalactopyranoside (IPTG) to a final concentration of 1 mM and incubated at 30°C for 6 h. The bacterial pellets were collected by centrifugation at 5,000 × g at 4°C for 20 min.

The recombinant HuscFvs were purified from the bacterial inclusion bodies (IBs) as described previously (Jittavisutthikul et al., 2016). Two grams of *E. coli* wet cell pellets were resuspended in 10 ml of BugBuster™ protein extraction reagent (Novagen, Schwalbach, Germany) and 20 µl of Lysonase™ bioprocessing reagent (Novagen) were added to each preparation. The preparations were kept at 25°C on a rotator for 20 min and cell pellets were collected after centrifugation at 8,000 × g at 4°C for 30 min. The IBs were washed with Wash-100 reagent [50 mM sodium phosphate buffer, pH 8.0; 500 mM NaCl; 5 mM EDTA; 8% (w/v) glycerol; and 1% (v/v) Triton X-100] twice and once with Wash-114 buffer [50 mM Tris-HCl, pH 8.0; 300 mM NaCl; and 1% (v/v) Triton X-114] with shaking at high speed for 40 min, and the IB pellets were then collected. The IBs were then washed with Wash-Solvent solution [50 mM Tris-HCl, pH 8.0; and 60% (v/v) isopropanol] and sterile ultrapure distilled water on ice, also with vigorous shaking, and centrifuged. Thereafter, 2.5 mg of purified IB pellets were solubilized in 5 ml of solubilizing buffer [50 mM CAPS, pH 11.0; 0.3% (w/v) *N*-lauryl sarcosine; and 1 mM dithiothreitol (DTT)] and kept at 4°C for 16 h. After dissolving completely, the protein was loaded into Snakeskin dialysis tubing with a molecular weight cut-off of 10 kDa (Thermo Fisher Scientific), and dialyzed against 750 ml of refolding buffer (20 mM imidazole, pH 8.5, supplemented with 0.1 mM DTT) at 4°C with slow stirring. After 3 h, the buffer was changed to a fresh refolding buffer, and dialysis was continued for 16 h. The refolded protein was subsequently dialyzed against a dialysis buffer without DTT with slow stirring at 4°C for 16 h. Each preparation was filtered through a 0.2-µm low protein binding Acrodisc® Syringe Filter (Pall, Port Washington, NY, United States) and kept at 30°C in a water bath for 3 h before adding 60 mM trehalose. The protein concentration of the refolded HuscFvs was determined using Pierce® BCA Protein Assay, while the quality and purity of the recombinant proteins were analyzed by SDS-PAGE and stained with Coomassie Brilliant Blue G-250 (Bio-rad, Hercules, CA, United States). Refolded HuscFv preparations were concentrated using Amicon® Ultra 4 ml 3K centrifugal filter devices (Merck Millipore, Darmstadt, Germany) and stored at –20°C until use.

## Circular Dichroism

The buffer of the HuscFv preparations was changed to 20 mM sodium phosphate buffer, pH 8.5, at a protein concentration of 0.1 mg/ml, and the antibodies were subjected to CD measurement. The data were recorded using a JASCO spectrometer (model J-815) equipped with a Peltier temperature controller system (Jasco, Tokyo, Japan) in a 1 mm path-length quartz cuvette. The proteins were scanned at 50 nm/min



at 25°C. The CD spectra were collected over a wavelength range of 190–260 nm.

## Cell Line

Human cervical carcinoma, HeLa, cells were cultured in Dulbecco's Modified Eagle's Medium (DMEM; Gibco, Carlsbad, CA, United States) supplemented with 10% (v/v) fetal bovine serum (Hyclone, Novato, CA, United States) and 1% (v/v) penicillin-streptomycin (complete DMEM) at 37°C in a 5% CO<sub>2</sub> atmosphere.

## Determination of the Biocompatibility of the HuscFvs to Mammalian Cells

The monolayer of HeLa cells established in individual wells of a 24-well tissue culture plate ( $\sim 2 \times 10^5$  cells/well) were washed with sterile PBS, added with 2  $\mu$ M of individual HuscFv preparations in complete DMEM, and incubated at 37°C in 5% CO<sub>2</sub> atmosphere for 24 h. Cells in the medium alone served as a background control. After 24 h, the percent viability of cells of each treatment was analyzed using an FITC-Annexin V Apoptosis Detection Kit (BD Biosciences, San Jose, CA, United States) according to the manufacturer's protocols. The cells were washed with Dulbecco's phosphate-buffered saline (DPBS) and resuspended in binding buffer. Five microliters of Annexin V-FITC conjugate and 5  $\mu$ l of propidium iodide (PI) were added. After 15-min incubation at room temperature (25°C) in darkness, apoptotic cells were enumerated by flow cytometric analysis (BD LSRFortessa™, San Jose, CA, United States) using BD FACSDiva™ software (BD Biosciences). At least 20,000 events of single cells per sample were collected.

## Cellular Apoptosis Mediated by 3O-C12-HSL

HeLa cells ( $\sim 2 \times 10^5$  cells/well) were treated with various concentrations of 3O-C12-HSL, i.e., 10, 25, 50, 75, and 100  $\mu$ M. The background control comprised of cells incubated with medium alone. After incubation at 37°C in a CO<sub>2</sub> incubator for 18 h, the cells were harvested and subjected to Annexin V/PI binding assay, as described above.

## Neutralization of 3O-C12-HSL-mediated-Cytotoxicity by HuscFvs

Fifty micromolars of 3O-C12-HSL in 0.25% DMSO were mixed with various concentrations of individual HuscFv preparations (0.25, 0.5, 1.0, and 1.2  $\mu$ M) for 1 h before adding to HeLa cells ( $\sim 2 \times 10^5$  cells/well) and incubated at 37°C in a CO<sub>2</sub> incubator for 18 h. After incubation, the cells were collected, washed, double-stained with Annexin V-FITC and PI, and analyzed by flow cytometry, as described above. Three independent experiments were performed.

## Neutralization of 3O-C12-HSL-mediated Cell Cycle Arrest by HuscFvs

HeLa cells ( $\sim 2 \times 10^5$  cells/well) were treated with a mixture of 50  $\mu$ M 3O-C12-HSL and 1  $\mu$ M of individual HuscFvs for

18 h. HeLa cells exposed to medium alone served as a control. After incubation, cells were washed with ice-cold PBS, fixed in 70% ethanol, and kept at  $-20^\circ\text{C}$  overnight. Cells were then washed 3 times with ice-cold PBS and incubated in 500  $\mu$ l of stain solution [10  $\mu$ g/ml PI, 100  $\mu$ g/ml RNase, and 0.1% (v/v) Triton X-100 in DPBS, pH 7.4] at room temperature in darkness for 30 min. The DNA contents of the cells were measured, and cell cycle histograms/distributions were generated. Then, the percentage of cells in the sub-G1 phase was determined by flow cytometry (BD LSRFortessa™) using BD FACSDiva™ software (BD Biosciences), with at least 10,000 recorded events per sample.

## Analysis of Nuclear Damage by Fluorescence Staining

Nuclear damage was studied using 4',6-diamidino-2-phenylindole (DAPI) staining. Briefly, HeLa cells ( $1 \times 10^6$  cells) were seeded on a 22  $\times$  22 mm square coverslip (Menzel-Glaser, Braunschweig, Germany) in a 6-well plate (Costar, New York, NY, United States) and kept at 37°C in a 5% CO<sub>2</sub> incubator for 24 h. The culture medium was removed and the cells were replenished with complete DMEM containing a mixture of 3O-C12-HSL (50  $\mu$ M) and HuscFvs (2  $\mu$ M). After 18 h, the cells were washed and fixed with 4% (v/v) paraformaldehyde in PBS, permeabilized with 1% (v/v) Triton X-100 in PBS, blocked with 3% (w/v) bovine serum albumin (BSA) in PBS at room temperature for 30 min, then washed. The permeabilized cells were stained and mounted with DAPI (1:5,000) (Molecular Probes, Carlsbad, CA, United States) in the anti-fade mounting medium. DNA fragmentation and chromatin condensation were observed under a confocal microscope (Carl Zeiss Laser Scanning System LSM 700, Jena, Germany). Images were processed using the Zeiss LSM Image Browser (version 6.0.0.309).

## Transmission Electron Microscopy

Transmission electron microscopy (TEM) was used to examine the ultrastructural changes of the HeLa cell mitochondria after various treatments. The cells from each treatment group were fixed with 2.5% (v/v) glutaraldehyde in 0.1 M sucrose phosphate buffer (SPB) at room temperature for 1 h, washed three times with 0.1 M SPB, post-fixed with 1.0% (w/v) osmium tetroxide in the same buffer for 1 h, and dehydrated with a graded series of ethanol. The dehydrated cells were infiltrated with pure LR white embedded medium (EMS®, Hatfield, PA, United States) in 70% (v/v) ethanol, embedded in a capsule beam, and incubated at 65°C for 48 h. The ultrathin (100 nm) sections of the cells were prepared; the sections were positioned on a 200 square-mesh copper grid and stained with ethanolic uranyl acetate and lead citrate. The morphological and structural characteristics of mitochondria were observed under a transmission electron microscope (model HT7700, Hitachi, Tokyo, Japan).

## Statistical Analysis

Statistical analyses of all experiments were performed using GraphPad Prism 5 software (La Jolla, CA, United States). One-way ANOVA followed by Tukey's *post hoc* multiple comparison tests were used to analyze the differences between groups. All data

are shown as mean  $\pm$  SD. Statistically significant difference was set at  $p < 0.05$ .

## RESULTS

### HuscFvs to 3O-C12-HSL

The refined models of HuscFvs for the selected HB2151 *E. coli* clones derived from phage biopanning with *P. aeruginosa* exotoxin A revealed that HuscFvs of three *E. coli* clones, i.e., E44 (HuscFv-E44), F15 (HuscFv-F15), and F19 (HuscFv-F19), showed reliable Ramachandran plots. The percent residues in the most favored regions, the additional allowed regions, the generously allowed regions, and the disallowed regions of the Ramachandran diagrams of the HuscFv-E44, HuscFv-F15, and HuscFv-F19 were 90.1, 6.8, 1.0, and 2.1 %; 91.3, 7.7, 0.5, and 0.5%; and 88.2, 9.4, 1.0, and 1.5%, respectively (Supplementary Figure S1).

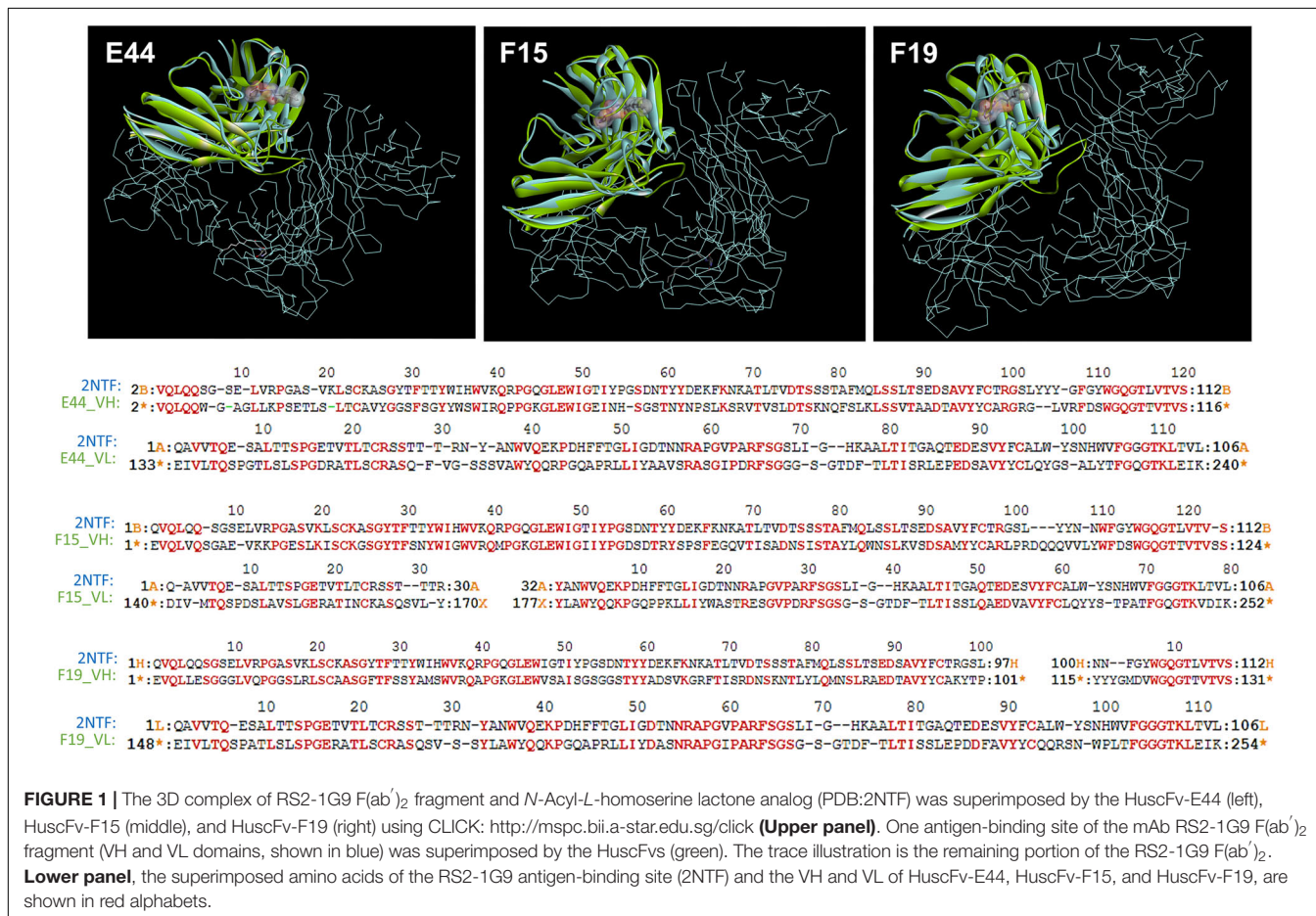
From structural comparisons of individual HuscFvs with the antigen-binding site of the well-characterized quorum quenching mAb, i.e., RS2-1G9 (shown previously to bind to and neutralize the activities of *P. aeruginosa* 3O-C12-HSL), it was found that the binding pockets of the three HuscFvs were superimposed with the antigen-binding site of RS2-1G9. The

coverage percentages of the overlapping structures between the modeled HuscFv-E44, HuscFv-F15, and HuscFv-F19 and the RS2-1G9 were 90.83, 89.29, and 88.58%, respectively (Figure 1 and Supplementary Table S1).

### Homology Modeling and Intermolecular Docking Between HuscFvs and 3O-C12-HSL

*In silico* intermolecular docking was performed to investigate the interaction of the HuscFvs with the 3O-C12-HSL. The residues of HuscFv-E44, HuscFv-F15, and HuscFv-F19 that tentatively formed interactive bonds with the haptenic 3O-C12-HSL target are shown in Figure 2 and Table 1. The Gibbs free energy ( $\Delta G$ ) of the representative complexes of respective HuscFvs with the ligand were  $-5.6$ ,  $-5.8$ , and  $-5.4$  kcal/mol, respectively.

The HuscFv-E44 used residues from VH-CDR2 and VL-CDR3, as well as help from VH-FR2, VH-FR3, VL-FR1, and VL-FR4 to form contact interfaces with the functional groups of 3O-C12-HSL. The interactions were three hydrogen bonds between L45 of VH-FR2 with the NH group of the coordinated 3O-C12-HSL (2.18 Å) and N60 of VH-CDR2, and W47 of VH-FR2 with the 3O-C12-HSL carbonyl oxygen of 3-oxo-group of the acyl chain (2.97 and 2.44 Å, respectively). There was one



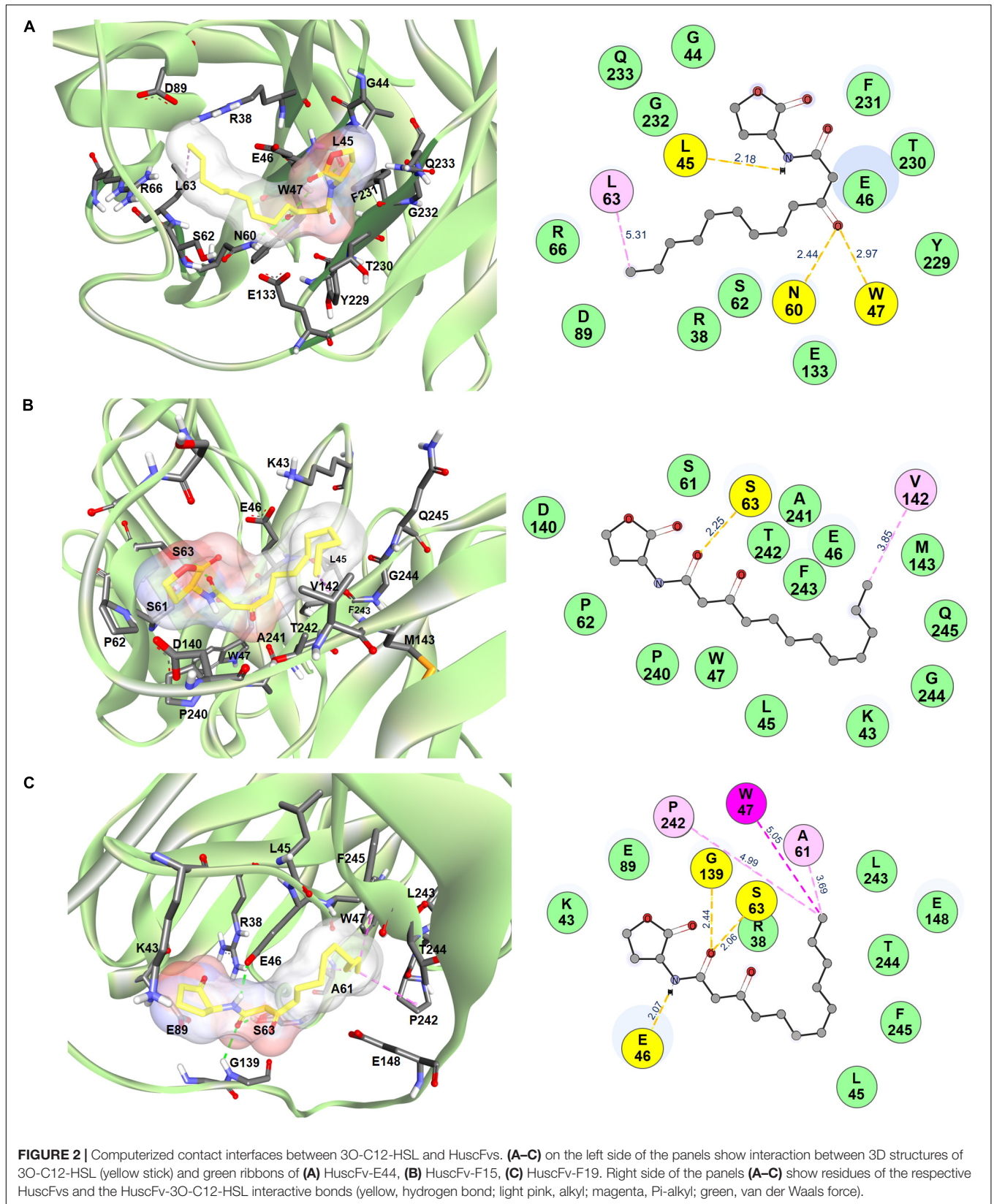




**TABLE 1 |** Residues of *Pseudomonas aeruginosa* 3O-C12-HSL predicted to form contact interfaces with the effective HuscFv-E44, HuscFv-F15, and HuscFv-F19.

3O-C12-HSL position	HuscFv-E44		Interactive bond
	Residue (s)	Domain	
Ketone group of HSL ring	E46	VH-FR2	Van de Waals
C3 of HSL ring	G44	VH-FR2	Van de Waals
	G232	VL-FR4	Van de Waals
C4 of HSL ring	G44	VH-FR2	Van de Waals
NH-group	L45	VH-FR2	Hydrogen
	E46	VH-FR2	Van de Waals
	F231	VL-FR4	Van de Waals
1-oxo-group	T230	VL-CDR3	Van de Waals
	F231	VL-FR4	Van de Waals
C2 of acyl chain	E46	VH-FR2	Van de Waals
	T230	VL-CDR3	Van de Waals
3-oxo-group	W47	VH-FR2	Hydrogen
	N60	VH-CDR2	Hydrogen
	E46	VH-FR2	Van de Waals
	Y229	VL-CDR3	Van de Waals
	E133	VL-FR1	Van de Waals
C5 of acyl chain	E133	VL-FR1	Van de Waals
C9 of acyl chain	S62	VH-CDR2	Van de Waals
C10, C11 of acyl chain	R38	VH-FR2	Van de Waals
	R66	VH-FR3	Van de Waals
C12 of acyl side chain	L63	VH-CDR2	Hydrophobic (alkyl)
C12 of acyl side chain	R38	VH-FR2	Van de Waals
	R66	VH-FR3	Van de Waals
	N89	VH-FR3	Van de Waals

3O-C12-HSL position	HuscFv-F15		Interactive bond
	Residue(s)	Domain	
C3 of HSL ring	P62	VH-CDR2	Van de Waals
C3, C4 of HSL ring	D140	VL-FR1	Van de Waals
1-oxo-group	W47	VH-FR2	Van de Waals
	S61	VH-CDR2	Van de Waals
	S63	VH-CDR2	Hydrogen
C2 of acyl chain	W47/A241	VH-FR2	Van de Waals
3-oxo-group	P240/A241/T242	VL-CDR3	Van de Waals
	W47	VH-FR2	Van de Waals
	A241	VL-CDR3	Van de Waals
C4 of acyl chain	W4	VH-FR2	Van de Waals
	F243	VL-FR4	Van de Waals
C5 of acyl chain	A241/T242	VL-CDR3	Van de Waals
	E46, W47	VH-FR2	Van de Waals
C6 of acyl chain	F243	VL-FR4	Van de Waals
C7 of acyl chain	L45, E46	VH-FR2	Van de Waals
	F243	VL-FR4	Van de Waals
C8 of acyl chain	K43, E46	VH-FR2	Van de Waals
C9 of acyl chain	K43	VH-FR2	Van de Waals
	F243/G244/Q245	VL-FR4	Van de Waals
C10 of acyl chain	F243/G244/Q245	VL-FR4	Van de Waals
C12 of acyl chain	V142	VL-FR1	Hydrophobic (alkyl)
	M143	VL-FR1	Van de Waals
	T242	VL-CDR3	Van de Waals
	F243	VL-FR4	Van de Waals

(Continued)

**TABLE 1 |** Continued

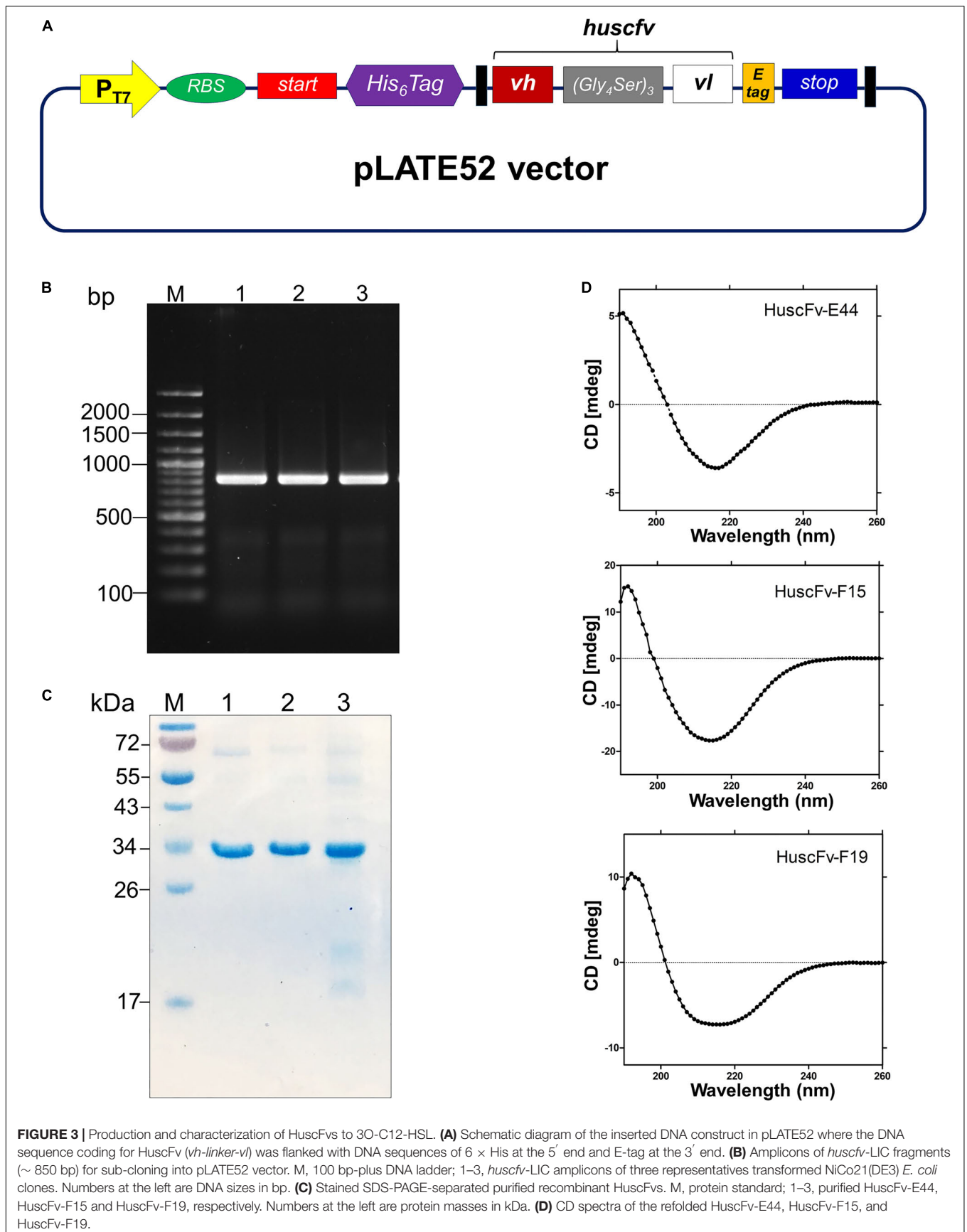
3O-C12-HSL position	HuscFv-F19		Interactive bond
	Residue(s)	Domain	
Ketone group of HSL ring	R38	VH-FR2	Van de Waals
	E89	VH-FR3	Van de Waals
C3, C4 of HSL ring	K43	VH-FR2	Van de Waals
Oxygen of HSL ring	E89	VH-FR3	Van de Waals
NH-group	R38, E46	VH-FR2	Hydrogen
	R38	VH-FR2	Van de Waals
1-oxo-group	S63	VH-CDR2	Hydrogen
	G139	Linker	Hydrogen
C2 of acyl side chain	R38	VH-FR2	Van de Waals
C7, C8 of acyl chain	L45	VH-FR2	Van de Waals
	F245	VL-FR4	Van de Waals
	T244	VL-CDR3	Van de Waals
C9 of acyl side chain	F245	VL-FR4	Van de Waals
	E148	VL-FR1	Van de Waals
C10 of acyl chain	E148	VL-FR1	Van de Waals
C11 of acyl chain	L243	VL-CDR3	Van de Waals
	W47	VH-FR2	Hydrophobic ( $\pi$ -alkyl)
C12 of acyl chain	A61	VH-CDR2	Hydrophobic (alkyl)
	P242	VL-CDR3	Hydrophobic (alkyl)

hydrophobic interaction (alkyl) formed between L63 of VH-CDR2 and C12 of the acyl chain of AHL. HuscFv-E44 also used many residues in different domains to form contact interfaces via van der Waals forces with the 3O-C12-HSL, including S62 of VH-CDR2; Y229 and T230 of VL-CDR3; R38, G44, and E46 of VH-FR2; R66 and D89 of VH-FR3, E133 of VL-FR1; and F231, G232, and Q233 of VL-FR4 (Table 1).

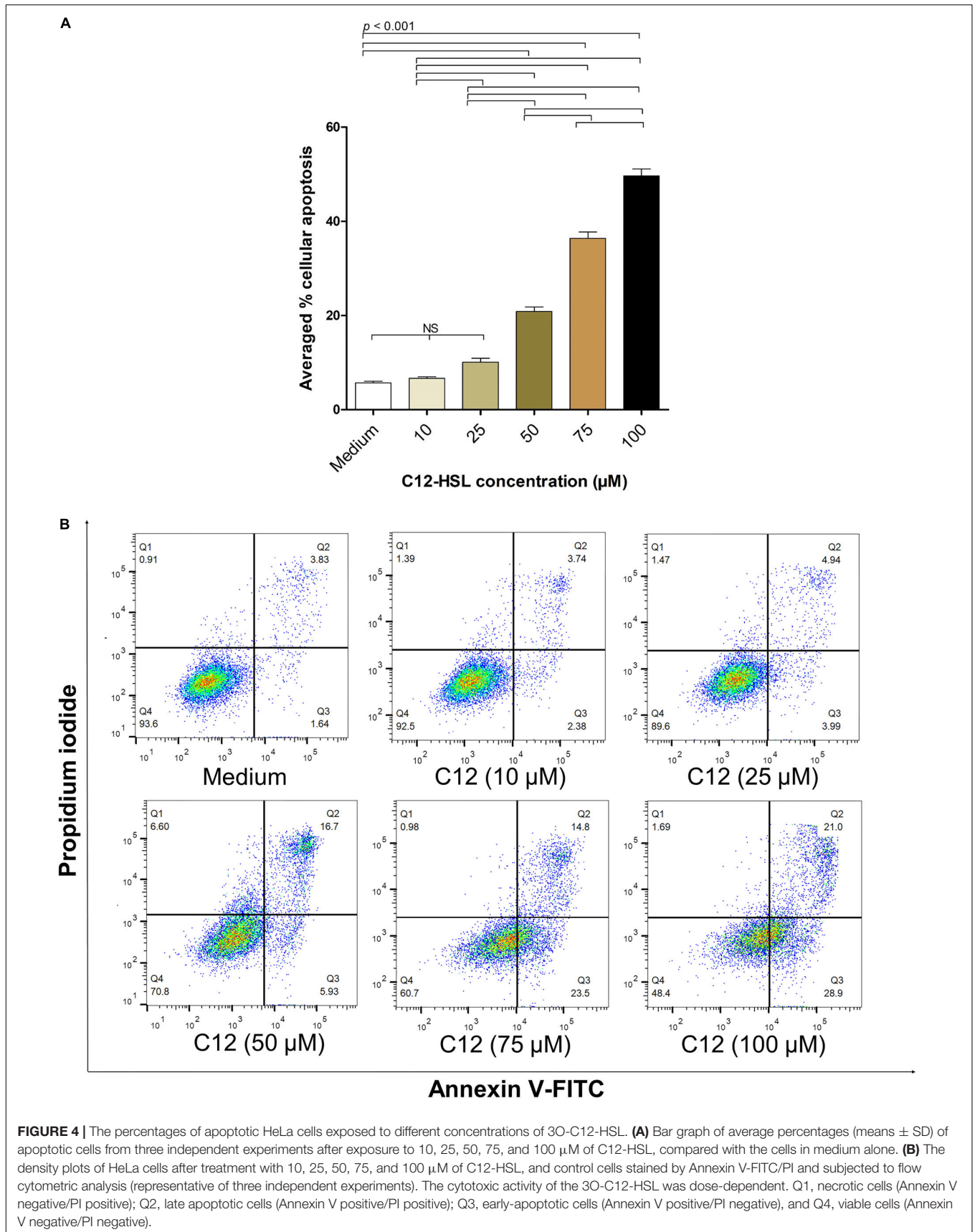
HuscFv-F15 formed a hydrogen bond (2.25 Å) with the carbonyl oxygen of the 1-oxo-group of the fatty acid-like ligand through S63 of VH-CDR2. This antibody also used V142 of VL-FR1 to form hydrophobic contact (alkyl) with the C12 of the hapten acyl chain. Several other positions of the 3O-C12-HSL molecule have interacted via van der Waals forces with several residues of the HuscFv-F15 including S61 and P62 of VH-CDR2; P240, A241, and T242 of VL-CDR3; K43, L45, E46, and W47 of VH-FR2; D140 and M143 of VL-FR1; and F243, G244, and Q245 of VL-FR4.

Serine 63 of VH-CDR2 and G139 of the HuscFv-F19 linker formed contact with the carbonyl oxygen of the 1-oxo-group of the 3O-C12-HSL via hydrogen bonds (2.06 and 2.44 Å, respectively). Hydrogen bonding also occurred between E46 of VH-FR2 and the NH-group of the HSL backbone (2.07 Å). The last carbon atom of the long acyl side chain of the 3O-C12-HSL formed  $\pi$ -alkyl hydrophobic interaction with W47 of VH-FR2 as well as the alkyl hydrophobic interaction with A61 of VH-CDR2 and P242 of VL-CDR3. In addition, the HuscFv-F19 formed van der Waals contacts with the 3O-C12-HSL by using L243 and T244 of VL-CDR3; R38, K43, and L45 of VH-FR2; E89 of VH-FR3; E148 of VL-FR1; and F245 of VL-FR4.

The results of the structural comparison of the HuscFvs with the quorum quenching mAb, RS2-1G9, and the intermolecular docking between the HuscFvs and the 3O-C12-HSL enticed us







to test further the ability of HuscFvs to neutralize *P. aeruginosa* 3O-C12-HSL activities.

## Large-Scale Production of HuscFvs

The *huscfv* inserts in the pCANTAB5E phagemids of the *E. coli* clones E44, F15, and F19 were sub-cloned into the pLATE52 vector. The DNA construct in the vector is shown in **Figure 3A**. The amplicon of DNA coding for 6 × His tagged-HuscFv formed a PCR amplicon band at ~ 850 bp, as revealed on agarose gel (**Figure 3B**). The refolded and purified HuscFv-E44, HuscFv-F15, and HuscFv-F19, with molecular sizes of about 34 kDa, are shown in **Figure 3C**.

Secondary structures of the refolded HuscFvs were determined by far-UV CD spectroscopy. The far-UV CD spectra (190–260 nm) for all HuscFvs revealed their  $\beta$ -sheet structures, which shared a similar CD spectra pattern (**Figure 3D**). The antibody preparations did not form aggregates.

## Biocompatibility of HuscFvs to Mammalian Cells

HeLa cells exposed to 2  $\mu$ M of HuscFv-E44, HuscFv-F15, and HuscFv-F19 for 24 h showed more than 90% viability, which was not different from the cells in medium alone ( $p > 0.05$ ) (**Supplementary Figure S2**) indicating biocompatibility of the HuscFvs to the representative mammalian cells.

## HuscFvs-bound 3O-C12-HSL Had Impairment in Inducing Mammalian Cell Apoptosis

The average percentages of apoptotic HeLa cells treated with 10, 25, 50, 75, and 100  $\mu$ M of 3O-C12-HSL dissolved in 0.25% DMSO, from three independent experiments, were  $6.67 \pm 0.53$ ,  $10.08 \pm 1.41$ ,  $20.85 \pm 1.62$ ,  $36.37 \pm 2.32$ , and  $49.63 \pm 2.51\%$ , respectively, while the background apoptotic cells of the control (cells in culture medium) was  $5.71 \pm 0.59\%$  (**Figure 4A**). **Figure 4B** shows the results of the flow cytometric analysis of apoptotic cells (stained with Annexin V/PI) from one representative experiment. The background apoptotic cells (% cell viability) with and without 0.25% DMSO in the culture medium were not different (**Supplementary Figure S3**).

The percentages of apoptotic HeLa cells exposed to 50  $\mu$ M of HuscFv-bound 3O-C12-HSL (0.25, 0.5, 1.0, and 1.2  $\mu$ M of individual HuscFvs) were significantly decreased compared with those without HuscFvs (**Table 2** and **Figure 5**). The HuscFvs of all three *E. coli* clones could neutralize 3O-C12-HSL, leading to reduced HeLa-cell apoptosis.

## HuscFv-bound-C12-HSL Had Reduced Ability to Induce sub-G1 Arrest of HeLa Cells

Exposure of HeLa cells with 50  $\mu$ M 3O-C12-HSL for 18 h resulted in  $3.79 \pm 0.52\%$  of apoptotic cells in the hypodiploid DNA peak (sub-G1 population, which were apoptotic cells) as determined by flow cytometric analysis of the PI-stained cellular DNA. The numbers of cells with a hypodiploid DNA peak induced

**TABLE 2** | Flow cytometric results evaluating the efficacy of HuscFvs using Annexin V-FITC/PI staining for 3O-C12-HSL-mediated cell apoptosis.

HeLa cells treated with	Percent cellular apoptosis	Percent cellular survival
Medium alone	6.77 $\pm$ 0.20	92.50 $\pm$ 0.28
3O-C12-HSL (50 $\mu$ M)	21.05 $\pm$ 2.23	72.15 $\pm$ 1.91
3O-C12-HSL + HuscFv-E44 (0.25 $\mu$ M)	15.03 $\pm$ 0.49	83.57 $\pm$ 0.50
3O-C12-HSL + HuscFv-E44 (0.5 $\mu$ M)	13.31 $\pm$ 0.12	85.33 $\pm$ 0.25
3O-C12-HSL + HuscFv-E44 (1.0 $\mu$ M)	12.99 $\pm$ 0.41	86.10 $\pm$ 0.35
3O-C12-HSL + HuscFv-E44 (1.2 $\mu$ M)	11.74 $\pm$ 0.66	87.30 $\pm$ 0.70
3O-C12-HSL + HuscFv-F15 (0.25 $\mu$ M)	16.04 $\pm$ 1.06	82.07 $\pm$ 1.20
3O-C12-HSL + HuscFv-F15 (0.5 $\mu$ M)	12.31 $\pm$ 0.49	85.97 $\pm$ 0.50
3O-C12-HSL + HuscFv-F15 (1.0 $\mu$ M)	12.88 $\pm$ 0.75	86.27 $\pm$ 0.75
3O-C12-HSL + HuscFv-F15 (1.2 $\mu$ M)	12.88 $\pm$ 0.48	85.53 $\pm$ 0.47
3O-C12-HSL + HuscFv-F19 (0.25 $\mu$ M)	13.53 $\pm$ 0.46	84.27 $\pm$ 0.49
3O-C12-HSL + HuscFv-F19 (0.5 $\mu$ M)	12.93 $\pm$ 0.18	85.80 $\pm$ 0.17
3O-C12-HSL + HuscFv-F19 (1.0 $\mu$ M)	10.71 $\pm$ 0.60	88.67 $\pm$ 0.64
3O-C12-HSL + HuscFv-F19 (1.2 $\mu$ M)	10.63 $\pm$ 0.91	88.60 $\pm$ 0.87

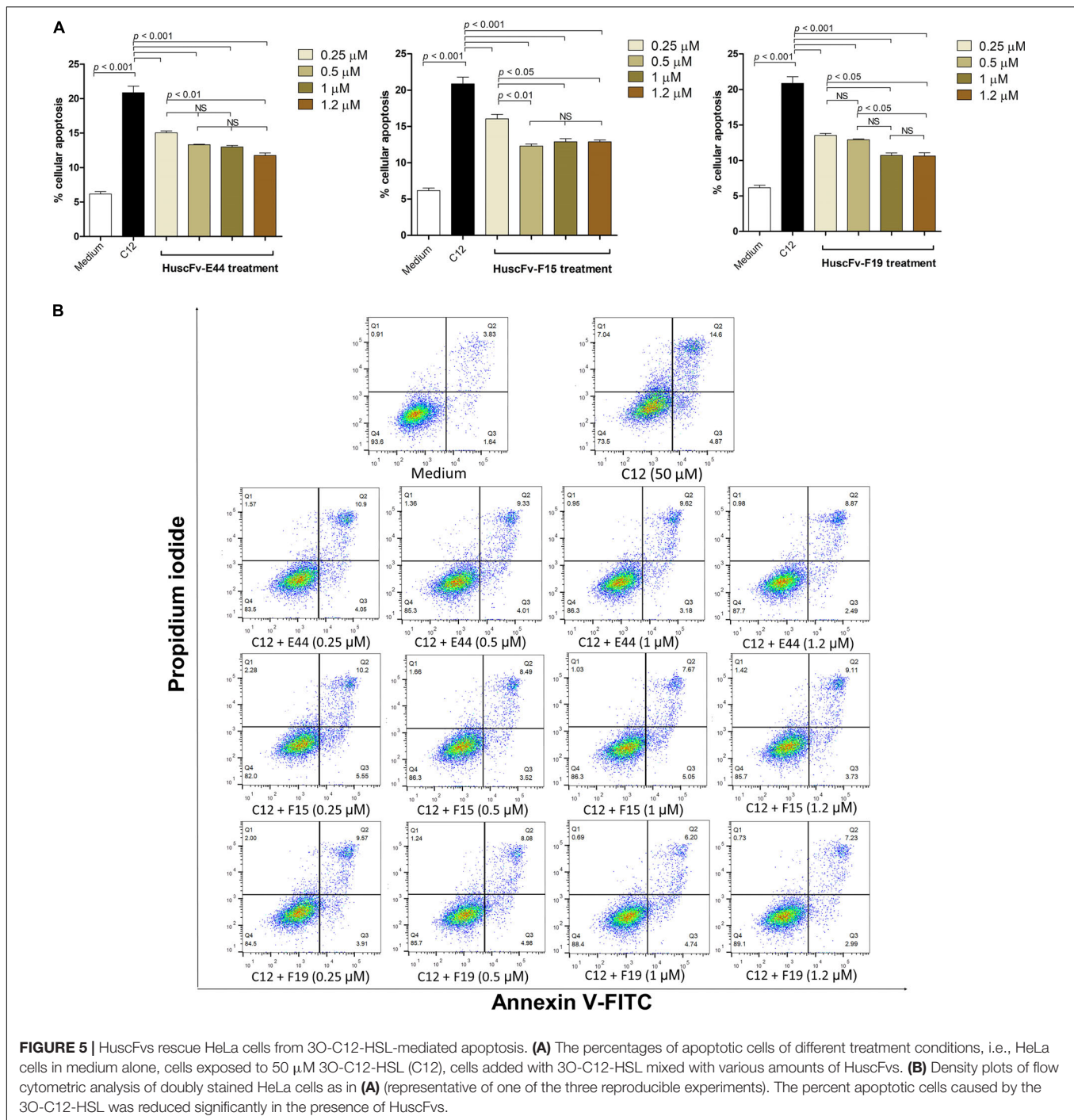
by the 3O-C12-HSL bound by the HuscFv-E44, HuscFv-F15, and HuscFv-F19, were decreased to  $2.58 \pm 0.10$ ,  $2.71 \pm 0.10$ , and  $1.79 \pm 0.11\%$ , respectively. The cells in medium alone had  $1.04 \pm 0.04\%$  apoptotic cells (**Figure 6**). The results of the sub-G0/G1 analysis were conformed to those of the Annexin V/PI binding assay data.

## Degrees of Nuclear Damage Mediated by HuscFv-bound 3O-C12-HSL

DAPI staining and confocal microscopy were used to observe the intact HeLa nuclei and nuclear DNA damage induced by the 3O-C12-HSL and the HuscFv-bound 3O-C12-HSL (**Figure 7**). Intact nuclei of normal HeLa cells were stained weakly by the dye (**Figure 7A**), while the fragmented nuclei of the 3O-C12-HSL-exposed cells were stained brightly (**Figure 7B**). Damage to the nuclear DNA was reduced in cells exposed to HuscFv-F19-bound 3O-C12-HSL, as shown by the dimly stained nuclei (**Figure 7C**).

## Mitigation of the 3O-C12-HSL Induced-mitochondrial Injuries by HuscFvs

Transmission electron microscopy was used to study mitochondrial changes of the HeLa cells after exposure to the 3O-C12-HSL and HuscFv-bound 3O-C12-HSL, using the cells in medium alone as a normal control. As shown in **Figures 8A,B**, the mitochondria of the normal cells revealed an intact mitochondrial subcellular structure. In contrast, mitochondria of the cells treated with 50  $\mu$ M of 3O-C12-HSL for 18 h exhibited a swollen appearance, with single or multiple distensions of the intercellular matrix in association with severe loss of cristae and double membranes (**Figures 8C,D**). The pathological changes of the mitochondria were ameliorated in the cells exposed to HuscFv-F19-bound 3O-C12-HSL (representative), i.e., mild mitochondrial swelling and more cristae (**Figures 8E,F**), compared with the 3O-C12-HSL-exposed cells.

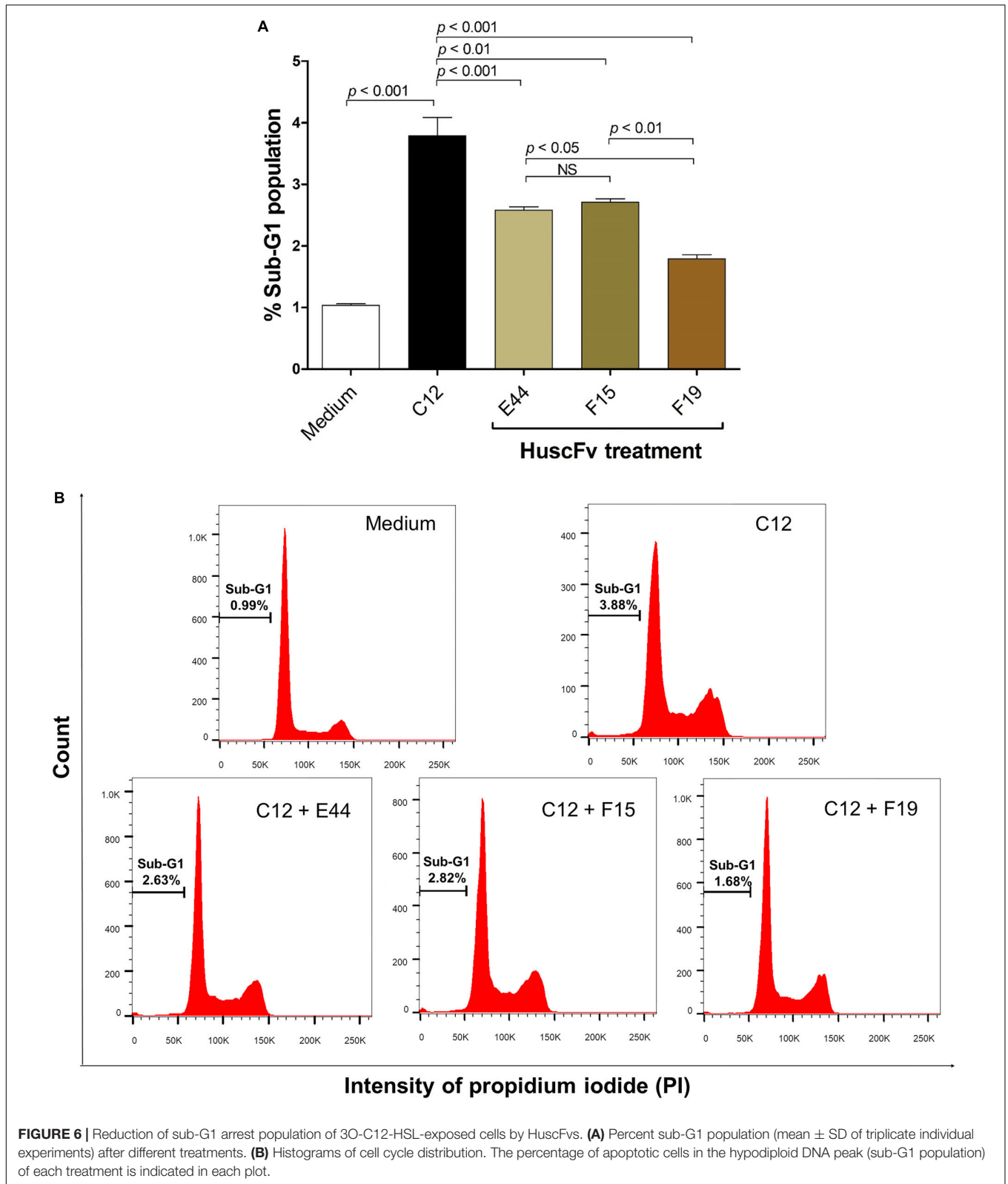


## DISCUSSION

*Pseudomonas aeruginosa* 3O-C12-HSL not only regulates virulence factors of the bacteria, but also causes inflammation in the infecting host by the induction of pro-inflammatory cytokine and chemokine synthesis (Smith et al., 2002). The 3O-C12-HSL killed mammalian cells through programmed cell death, i.e., an apoptotic mechanism at concentrations ranging from 10 to 100 μM by rapidly triggering depolarization of

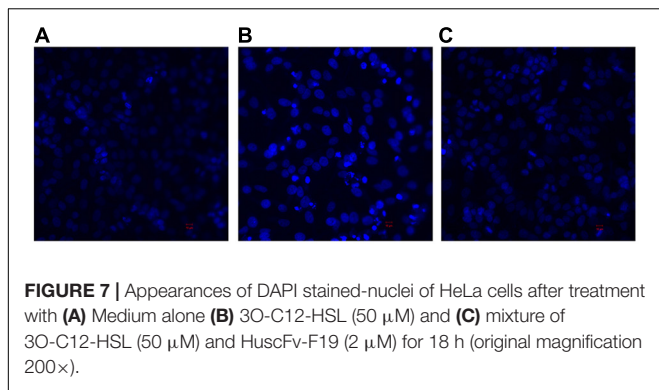
mitochondrial membrane potential and release of cytochrome *c* into cytosol, which activates the caspase cascades (Sultan and Sokolove, 2001; Tateda et al., 2003; Kravchenko et al., 2006; Schwarzer et al., 2012; Tao et al., 2016, 2018). The apoptotic cells manifest mitochondrial permeability transition (MPT), caspase activation, nuclear fragmentation, phosphatidylserine externalization, and cell shrinkage with apoptotic bodies (Wyllie et al., 1980; Cummings and Schnellmann, 2004). Mitochondrial swelling, depolarization, and membrane permeability are the





key markers of the MPT that indicates mitochondria-stimulated programmed cell death in the pathogenesis of several diseases. Upon response to external stimuli or oxidative stress, the

cells undergo continuous opening of permeability transition pores (PTP) in the mitochondrial inner membrane, which augments colloidal osmotic pressure in the matrix together



with mitochondrial membrane depolarization, resulting in mitochondrial swelling (Chapa-Dubocq et al., 2018) followed by rupture of the mitochondrial outer membrane and release of cytochrome *c* into the cytosol and activation of caspase cascades (Petronilli et al., 2001). The stimulated caspase-3 activates endogenous endonuclease, which cleaves nuclear DNA (Zhang and Ming, 2000). Cells with apoptotic fragmented DNA or sub-G1 population are used as a marker of apoptosis (Riccardi and Nicoletti, 2006). In this study, 3O-C12-HSL produced a significant dose-dependent increment in mammalian cell death by inducing apoptosis, which validates previous notions on the cytotoxicity of *P. aeruginosa* QS substance.

Deletion of *lasI* or *lasI* and *rhlI* diminished the lung-colonization ability of *P. aeruginosa* in a mouse model of acute pneumonitis (Smith et al., 2002). *P. aeruginosa* mutants with defective QS are known to have less virulence and be more susceptible to antibiotic treatments and host immunity than the respective wild-type (Hentzer et al., 2003). As such, *P. aeruginosa* QS systems are attractive targets for direct-acting therapeutic agents, of which the expected treatment consequences are mitigation of the severity of the bacteria-associated diseases (Penesyan et al., 2015). During the past decades, several groups of *P. aeruginosa* QS inhibitors/modulators have been identified: small chemical molecules, i.e., AHL analogs (phenylpropionyl homoserine lactones and phenylloxycetyl homoserine lactones of the *N*-aryl homoserine lactone library) (Geske et al., 2008), *N*-acyl cyclopentylamides (Ishida et al., 2007), halogenated furanone compound (Hentzer et al., 2002), other furanone derivatives (Kim et al., 2008), aspirin (El-Mowafy et al., 2014), and itaconimides and citraconimides (Fong et al., 2018); and natural inhibitors, such as secondary metabolites of the Australian marine macroalgae, *Delisea pulchra* (Givskov et al., 1996), patulin and penicillic acid from extracts of *Penicillium* species (Rasmussen et al., 2005), an organosulfur compound found in garlic extracts, named Ajoene (Jakobsen et al., 2012), and derivatives of ellagic acid (dilactone of hexahydroxydiphenic acid) from black or chebulic myrobalan, *Terminalia chebula* Retz (Sarabhai et al., 2013). Unfortunately, these compounds are relatively toxic to mammalian cells, which limits their therapeutic use (Ni et al., 2009). Recently, natural plant-derived compounds, *trans*-cinnamaldehyde (CA), and salicylic acid (SA) have been shown to effectively downregulate both *las* and *rhl*

QS systems, reduce the production of extracellular virulence factors, i.e., protease, elastase, and pyocyanin, and reduce biofilm formation, concomitantly with repressed rhamnolipid gene expression (Ahmed et al., 2019). However, the sole use of QS inhibitors at high concentrations to eradicate bacterial infection completely is of legitimate concern due to potential toxicity (Shreaz et al., 2016).

Passive immunization has been used as an intervention for post-exposure morbidity and/or treatment of diseases since the late 18th century (Keller and Stiehm, 2000). An antibody molecule uses multiple amino acid residues in several CDRs (sometimes with the help of FRs) to form multiple non-covalent bonds with the target molecule, thus, making it difficult for pathogens to create antibody escape mutants, compared with small molecular drugs/inhibitors, from which resistant variants emerge rather easily and frequently. Therapeutic antibodies may be in the form of intact molecules (two antigen-binding sites with Fc fragment- when the bioactivities of the Fc are required for effectiveness) or merely smaller antibody fragments, i.e., F(ab')<sub>2</sub>, Fab, scFv, or single domain (VH, V<sub>H</sub>H) with higher tissue penetrating ability than the intact four-chain counterpart when the Fc is dispensable. For *P. aeruginosa* infection, specific murine mAb, RS2-1G9, directed toward bacterial 3O-C12-HSL has been generated for use as an immunotherapeutic agent (Kaufmann et al., 2006, 2008). This murine antibody displayed the cytoprotective effect of 3O-C12-HSL-exposed host cells (Kaufmann et al., 2006, 2008; Debler et al., 2007). In addition, sheep-mouse chimeric mAb recognized native AHL protected mice from lethal *P. aeruginosa* infection (Palliyil et al., 2014). Nevertheless, while these 3O-C12-HSL-specific antibodies have therapeutic potential, their immunogenicity in human recipients, with possible adverse consequences, such as serum sickness, should be of concern.

Nowadays, any engineered fully human antibody format can be generated *in vitro* using phage display technology, invented by Nobel laureate, George Pearson Smith (Smith, 1985) as a biological tool (Santajit et al., 2019). The target antigens, such as proteins or peptides, attached to a carrier surface, e.g., fixed cell, plastic bead, or well of an ELISA plate, can be used as bait to fish out phage clones that display recombinant antibodies binding to the antigen from an antibody phage display library (Kulkeaw et al., 2009). Suppressor *E. coli*, such as strain HB2151 transfected with antigen-bound phages, when grown in appropriate conditioned medium, produces antigen-specific antibodies, and these antibodies can be isolated from the bacterial lysate/homogenate (Glab-Ampai et al., 2017; Santajit et al., 2019). Nevertheless, attachment of the small molecular haptens, like 3O-C12-HSL, to solid surfaces (as well as retaining the native configuration of the molecule) for conventional phage biopanning, is a relatively complicated process compared with proteins or peptides. Therefore, in this study, an alternative method was used to produce fully human scFvs (HuscFvs) to the synthetic *P. aeruginosa* 3O-C12-HSL based on the principle of antibody polyspecificity and antigenic molecular mimicry, i.e., completely unrelated molecules can share common receptors, possibly through similar structural and/or chemical features involved in recognition and binding (Wing, 1995;



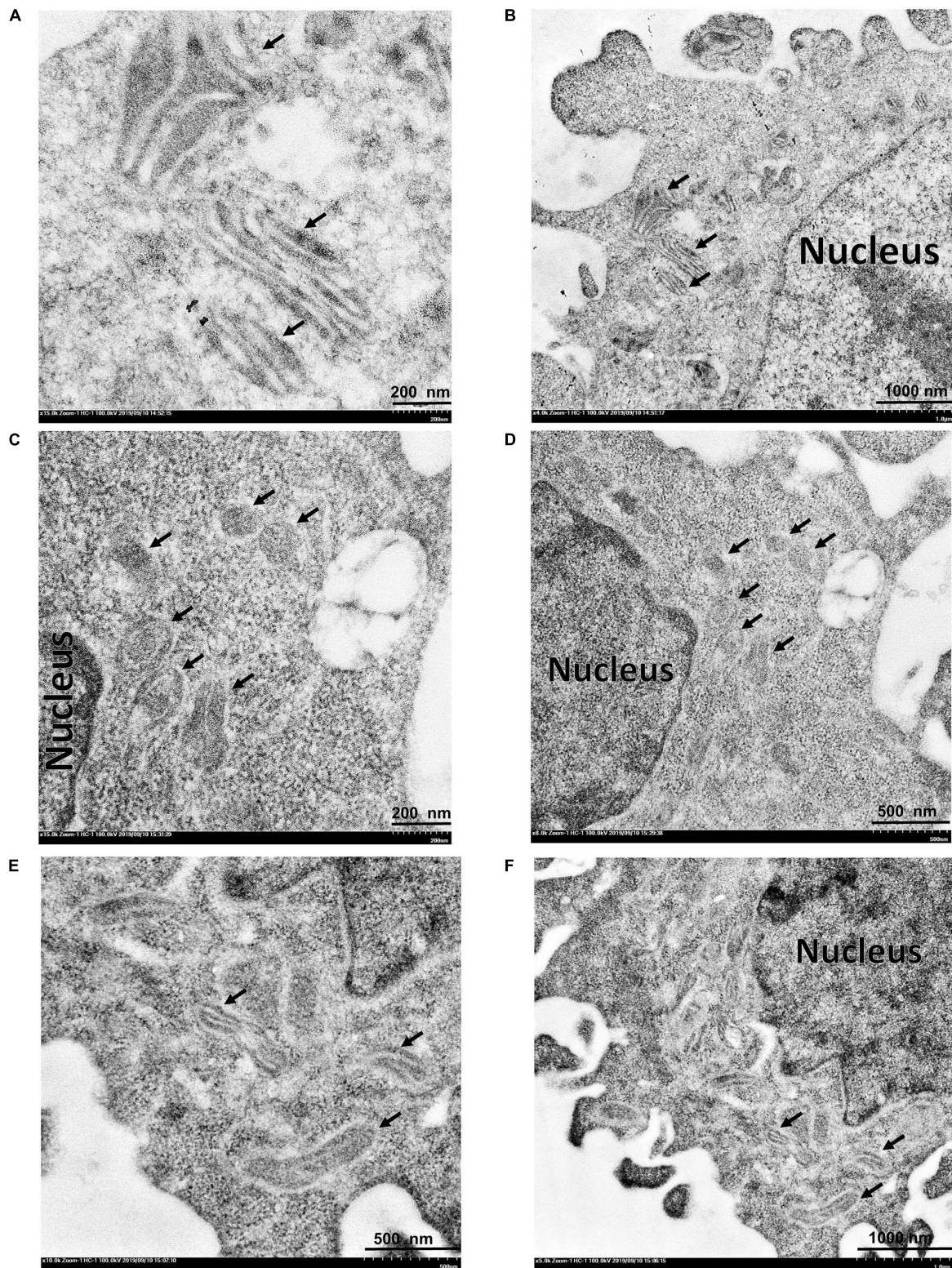


**FIGURE 8 |** Transmission electron micrographs of mitochondrial ultrastructure. **(A,B)** normal mitochondria of HeLa cells. **(C,D)** HeLa cells treated with 30-C12-HSL (50  $\mu$ M). **(E,F)** HeLa cells treated with a mixture of 50  $\mu$ M 30-C12-HSL and 2  $\mu$ M HuscFv-F19. Black arrows indicate mitochondria of the HeLa cells. Mitochondria of the cells exposed to the 30-C12-HSL were swollen, characterized by a size increment with decreased electron density of the crista-free matrix.



Tapryal et al., 2013). A repertoire of *E. coli* clones carrying recombinant *huscfv*-phagemids was previously retrieved from a HuscFv phage display library (Kulkeaw et al., 2009) by panning with *P. aeruginosa* exotoxin A (Santajit et al., 2019). Moreover, because the previously produced murine mAb, RS2-1G9, has been known as the *P. aeruginosa* quorum quencher, we used computerized antibody structure superimposition to select the bacterial derived-HuscFvs that shared structural homology with the murine mAb RS2-1G9 antigen-binding site. Using this method, the HuscFvs of three phagemid-transformed *E. coli* clones (E44, F15, and F19) showed high and satisfactory degrees of molecular similarity to the mAb RS2-1G9 antigen-binding site. Besides, these HuscFvs could neutralize the cytotoxic effects of the 3O-C12-HSL in the induction of cellular apoptosis. The HuscFv bound-3O-C12-HSL had a reduced capacity to mediate mitochondrial swelling, diminishing DNA damage and reducing sub-G1 arrest population of exposed cells. Unfortunately, the amount of C12-HSL inside the HeLa cells with and without HuscFv treatments were not measured; therefore, it is not known whether the HuscFvs could prevent HSL from entering the cells. Although the actual 3O-C12-HSL neutralizing mechanism of the HuscFvs needs laboratory investigation, the predicted structural complexes between the QS (ligand) and the HuScFvs (receptors) indicated that the latter used several residues in different CDRs and FRs to interact non-covalently with the target, including van der Waals' forces, hydrophobic interactions, and hydrogen bonds. These interactions might render the disarming of the bacterial toxic molecule through C12-HSL signal interference, which would mitigate bacterial disease severity. This perspective needs further testing of the HuscFvs on *P. aeruginosa* phenotypes both *in vitro* (bacterial culture), such as expression of the QS controlled virulence factors, as well as in the *in vivo* model of bacterial infection.

## CONCLUSION

The engineered human single-chain variable fragments that attenuated the potent cytotoxicity of the *P. aeruginosa* quorum sensing molecule, 3O-C12-HSL, were generated successfully through the molecular basis of antibody polyspecificity and antigenic mimicry. The fully human antibody fragments rescued mammalian cells from the 3O-C12-HSL-mediated mitochondrial injuries, DNA damage, and cellular apoptosis *in vitro*. They should be tested further by step-by-step *in vivo* toward the

clinical application as a sole or an adjunct therapy for the failing antibiotic treatment of *P. aeruginosa* infections.

## DATA AVAILABILITY STATEMENT

All datasets generated for this study are included in the article/**Supplementary Material**.

## AUTHOR CONTRIBUTIONS

NI and WC conceived the project, analyzed the data, and edited the manuscript. SS did most of the experiments, drafted the manuscript, and prepared the figures. KM helped SS with flow cytometric analysis. WS advised SS on recombinant HuscFv production. PP supervised SS on fluorescence staining and confocal microscopy. SA performed the electron microscopy. NS, OR, and MC-N helped NI and WC to analyze the data and made comments. All authors critically reviewed the manuscript and gave final approval for publication.

## FUNDING

This work was co-supported by the RSA scholar grant (RSA5980048) to NI, NSTDA Chair Professor grant (P-1450624) funded by the Crown Property Bureau of Thailand to WC, and Royal Golden Jubilee Ph.D. scholarship grant (PHD/0073/2558) to SS from the Thailand Research Fund.

## ACKNOWLEDGMENTS

We acknowledge the Center of Research Excellence on Therapeutic Proteins and Antibody Engineering, Department of Parasitology, and Biomedical Research Unit, Department of Research, Faculty of Medicine Siriraj Hospital, for their technical support.

## SUPPLEMENTARY MATERIAL

The Supplementary Material for this article can be found online at: <https://www.frontiersin.org/articles/10.3389/fmicb.2020.01172/full#supplementary-material>

## REFERENCES

- Abhinandan, K. R., and Martin, A. C. (2008). Analysis and improvements to Kabat and structurally correct numbering of antibody variable domains. *Mol. Immunol.* 45, 3832–3839. doi: 10.1016/j.molimm.2008.05.022
- Ahmed, S. A. K. S., Rudden, M., Smyth, T. J., Dooley, J. S., Marchant, R., and Banat, I. M. (2019). Natural quorum sensing inhibitors effectively downregulate gene expression of *Pseudomonas aeruginosa* virulence factors. *Appl. Microbiol. Biotechnol.* 103, 3521–3535. doi: 10.1007/s00253-019-09618-0
- Blevess, S., Soscia, C., Nogueira-Orlandi, P., Lazdunski, A., and Filloux, A. (2005). Quorum sensing negatively controls type III secretion regulon expression in *Pseudomonas aeruginosa* PAO1. *J. Bacteriol.* 187, 3898–3902. doi: 10.1128/jb.187.11.3898-3902.2005
- Boontham, P., Robins, A., Chandran, P., Pritchard, D., Cámara, M., Williams, P., et al. (2008). Significant immunomodulatory effects of *Pseudomonas aeruginosa* quorum-sensing signal molecules: possible link in human sepsis. *Clin. Sci.* 115, 343–351. doi: 10.1042/cs20080018
- Chapa-Dubocq, X., Makarov, V., and Javadov, S. (2018). Simple kinetic model of mitochondrial swelling in cardiac cells. *J. Cell. Physiol.* 233, 5310–5321. doi: 10.1002/jcp.26335
- Cummings, B. S., and Schnellmann, R. G. (2004). Measurement of cell death in mammalian cells. *Curr. Protoc. Pharmacol.* 25, 12–18.

- Debler, E. W., Kaufmann, G. F., Kirchdoerfer, R. N., Mee, J. M., Janda, K. D., and Wilson, I. A. (2007). Crystal structures of a quorum-quenching antibody. *J. Mol. Biol.* 368, 1392–1402. doi: 10.1016/j.jmb.2007.02.081
- Defoirdt, T., Boon, N., and Bossier, P. (2010). Can bacteria evolve resistance to quorum sensing disruption? *PLoS Pathog.* 6:e1000989. doi: 10.1371/journal.ppat.1000989
- Duan, K., and Surette, M. G. (2007). Environmental regulation of *Pseudomonas aeruginosa* PAO1 Las and Rhl quorum-sensing systems. *J. Bacteriol.* 189, 4827–4836. doi: 10.1128/jb.00043-07
- Eberhard, A., Burlingame, A. L., Eberhard, C., Kenyon, G. L., Neelson, K. H., and Oppenheimer, N. J. (1981). Structural identification of autoinducer of *Photobacterium fischeri* luciferase. *Biochemistry* 20, 2444–2449. doi: 10.1021/bi00512a013
- El-Mowafy, S. A., El Galil, K. H. A., El-Messery, S. M., and Shaaban, M. I. (2014). Aspirin is an efficient inhibitor of quorum sensing, virulence and toxins in *Pseudomonas aeruginosa*. *Microb. Pathog.* 74, 25–32. doi: 10.1016/j.micpath.2014.07.008
- Fong, J., Mortensen, K. T., Nørskov, A., Qvortrup, K., Yang, L., Tan, C. H., et al. (2018). Itaconimides as novel quorum sensing inhibitors of *Pseudomonas aeruginosa*. *Front. Cell. Infect. Microbiol.* 8:443. doi: 10.3389/fcimb.2018.00443
- Forli, S., Huey, R., Pique, M. E., Sanner, M. F., Goodsell, D. S., and Olson, A. J. (2016). Computational protein–ligand docking and virtual drug screening with the AutoDock suite. *Nat. Protoc.* 11, 905–919. doi: 10.1038/nprot.2016.051
- Geske, G. D., Mattmann, M. E., and Blackwell, H. E. (2008). Evaluation of a focused library of N-aryl L-homoserine lactones reveals a new set of potent quorum sensing modulators. *Bioorg. Med. Chem. Lett.* 18, 5978–5981. doi: 10.1016/j.bmcl.2008.07.089
- Givskov, M., de Nys, R., Manefield, M., Gram, L., Maximilien, R. I. A., Eberl, L. E. O., et al. (1996). Eukaryotic interference with homoserine lactone-mediated prokaryotic signalling. *J. Bacteriol.* 178, 6618–6622. doi: 10.1128/jb.178.22.6618-6622.1996
- Glab-Ampai, K., Chulanetra, M., Malik, A. A., Juntadech, T., Thanongsaksrikul, J., Srimanote, P., et al. (2017). Human single chain-transbodies that bound to domain-I of non-structural protein 5A (NS5A) of hepatitis C virus. *Sci. Rep.* 7:15042.
- Hentzer, M., Riedel, K., Rasmussen, T. B., Heydorn, A., Andersen, J. B., Parsek, M. R., et al. (2002). Inhibition of quorum sensing in *Pseudomonas aeruginosa* biofilm bacteria by a halogenated furanone compound. *Microbiology* 148, 87–102. doi: 10.1099/00221287-148-1-87
- Hentzer, M., Wu, H., Andersen, J. B., Riedel, K., Rasmussen, T. B., Bagge, N., et al. (2003). Attenuation of *Pseudomonas aeruginosa* virulence by quorum sensing inhibitors. *EMBO J.* 22, 3803–3815. doi: 10.1093/emboj/cdg366
- Ishida, T., Ikeda, T., Takiguchi, N., Kuroda, A., Ohtake, H., and Kato, J. (2007). Inhibition of quorum sensing in *Pseudomonas aeruginosa* by N-acyl cyclopentylamides. *Appl. Environ. Microbiol.* 73, 3183–3188. doi: 10.1128/aem.02233-06
- Jacobi, C. A., Schiffner, F., Henkel, M., Waibel, M., Stork, B., Daubrawa, M., et al. (2009). Effects of bacterial N-acyl homoserine lactones on human Jurkat T lymphocytes—O<sub>2</sub>DHL induces apoptosis via the mitochondrial pathway. *Int. J. Med. Microbiol.* 299, 509–519. doi: 10.1016/j.ijmm.2009.03.005
- Jakobsen, T. H., van Gennip, M., Phipps, R. K., Shanmugham, M. S., Christensen, L. D., Alhede, M., et al. (2012). Ajoene, a sulfur-rich molecule from garlic, inhibits genes controlled by quorum sensing. *Antimicrob. Agents Chemother.* 56, 2314–2325. doi: 10.1128/aac.05919-11
- Jittavisuthikul, S., Seesuay, W., Thanongsaksrikul, J., Thueng-in, K., Srimanote, P., Werner, R. G., et al. (2016). Human transbodies to HCV NS3/4A protease inhibit viral replication and restore host innate immunity. *Front. Immunol.* 7, 318. doi: 10.3389/fimmu.2016.00318
- Kalia, V. C., Wood, T. K., and Kumar, P. (2014). Evolution of resistance to quorum-sensing inhibitors. *Microb. Ecol.* 68, 13–23.
- Kaufmann, G. F., Park, J., Mee, J. M., Ulevitch, R. J., and Janda, K. D. (2008). The quorum quenching antibody RS2-1G9 protects macrophages from the cytotoxic effects of the *Pseudomonas aeruginosa* quorum sensing signaling molecule N-3-oxo-dodecanoyl-homoserine lactone. *Mol. Immunol.* 45, 2710–2714. doi: 10.1016/j.molimm.2008.01.010
- Kaufmann, G. F., Sartorio, R., Lee, S. H., Mee, J. M., Altobelli, L. J., Kujawa, D. P., et al. (2006). Antibody interference with N-acyl homoserine lactone-mediated bacterial quorum sensing. *J. Am. Chem. Soc.* 128, 2802–2803. doi: 10.1021/ja0578698
- Keller, M. A., and Stiehm, E. R. (2000). Passive immunity in prevention and treatment of infectious diseases. *Clin. Microbiol. Rev.* 13, 602–614. doi: 10.1128/cmr.13.4.602
- Kim, C., Kim, J., Park, H. Y., Park, H. J., Lee, J. H., Kim, C. K., et al. (2008). Furanone derivatives as quorum-sensing antagonists of *Pseudomonas aeruginosa*. *Appl. Microbiol. Biotechnol.* 80, 37–47.
- Kim, S., Thiessen, P. A., Bolton, E. E., Chen, J., Fu, G., Gindulyte, A., et al. (2015). PubChem substance and compound databases. *Nucleic Acids Res.* 44, D1202–D1213.
- Kravchenko, V. V., Kaufmann, G. F., Mathison, J. C., Scott, D. A., Katz, A. Z., Wood, M. R., et al. (2006). N-(3-oxo-acyl) homoserine lactones signal cell activation through a mechanism distinct from the canonical pathogen-associated molecular pattern recognition receptor pathways. *J. Biol. Chem.* 281, 28822–28830. doi: 10.1074/jbc.m606613200
- Krzyżek, P. (2019). Challenges and limitations of anti-quorum sensing therapies. *Front. Microbiol.* 10:2473. doi: 10.3389/fmicb.2019.02473
- Kulkeaw, K., Sakolvaree, Y., Srimanote, P., Tongtawe, P., Maneewatch, S., Sookkrung, N., et al. (2009). Human monoclonal ScFv neutralize lethal Thai cobra. *Naja kaouthia*, neurotoxin. *J. Proteomics* 72, 270–280.
- Laskowski, R. A., MacArthur, M. W., Moss, D. S., and Thornton, J. M. (1993). PROCHECK: a program to check the stereochemical quality of protein structures. *J. Appl. Crystallogr.* 26, 283–291. doi: 10.1107/s002188992009944
- Li, L., Hooi, D., Chhabra, S. R., Pritchard, D., and Shaw, P. E. (2004). Bacterial N-acylhomoserine lactone-induced apoptosis in breast carcinoma cells correlated with down-modulation of STAT3. *Oncogene* 23, 4894–4902. doi: 10.1038/sj.onc.1207612
- Liu, Y. C., Chan, K. G., and Chang, C. Y. (2015). Modulation of host biology by *Pseudomonas aeruginosa* quorum sensing signal molecules: messengers or traitors. *Front. Microbiol.* 6:1226. doi: 10.3389/fmicb.2015.01226
- López-Jacome, L. E., Garza Ramos-Martínez, G., Hernández-Durán, M., Franco-Cendejas, R., Loarca, D., Romero-Martínez, D., et al. (2019). AiiM lactonase strongly reduces quorum sensing controlled virulence factors in clinical strains of *Pseudomonas aeruginosa* isolated from burned patients. *Front. Microbiol.* 10:2657. doi: 10.3389/fmicb.2019.02657
- Maeda, T., García-Contreras, R., Pu, M., Sheng, L., García, L. R., Tomás, M., et al. (2012). Quorum quenching quandary: resistance to antivirulence compounds. *ISME J.* 6, 493–501. doi: 10.1038/ismej.2011.122
- Malhotra, S., Hayes, D., and Wozniak, D. J. (2019). Cystic fibrosis and *Pseudomonas aeruginosa*: the host-microbe interface. *Clin. Microbiol. Rev.* 32:e00138-18.
- Miyairi, S., Tateda, K., Fuse, E. T., Ueda, C., Saito, H., Takabatake, T., et al. (2006). Immunization with 3-oxododecanoyl-L-homoserine lactone-protein conjugate protects mice from lethal *Pseudomonas aeruginosa* lung infection. *J. Med. Microbiol.* 55, 1381–1387. doi: 10.1099/jmm.0.46658-0
- Moradali, M. F., Ghods, S., and Rehm, B. H. (2017). *Pseudomonas aeruginosa* lifestyle: a paradigm for adaptation, survival, and persistence. *Front. Cell. Infect. Microbiol.* 7:39. doi: 10.3389/fcimb.2017.00039
- Nguyen, M. N., Tan, K. P., and Madhusudhan, M. S. (2011). CLICK—topology-independent comparison of biomolecular 3D structures. *Nucleic Acids Res.* 39, W24–W28.
- Ni, N., Li, M., Wang, J., and Wang, B. (2009). Inhibitors and antagonists of bacterial quorum sensing. *Med. Res. Rev.* 29, 65–124. doi: 10.1002/med.20145
- O'Connor, G., Knecht, L. D., Salgado, N., Strobel, S., Pasini, P., and Daunert, S. (2015). Whole-cell biosensors as tools for the detection of quorum-sensing molecules: uses in diagnostics and the investigation of the quorum-sensing mechanism. *Adv. Biochem. Eng. Biotechnol.* 154, 181–200. doi: 10.1007/10\_2015\_337
- Palliyil, S., and Broadbent, I. D. (2009). Novel immunotherapeutic approaches to the treatment of infections caused by Gram-negative bacteria. *Curr. Opin. Pharmacol.* 9, 566–570. doi: 10.1016/j.coph.2009.07.007
- Palliyil, S., Downham, C., Broadbent, I., Charlton, K., and Porter, A. J. (2014). High-sensitivity monoclonal antibodies specific for homoserine lactones protect mice from lethal *Pseudomonas aeruginosa* infections. *Appl. Environ. Microbiol.* 80, 462–469. doi: 10.1128/aem.02912-13

- Pearson, J. P., Gray, K. M., Passador, L., Tucker, K. D., Eberhard, A., Iglewski, B. H., et al. (1994). Structure of the autoinducer required for expression of *Pseudomonas aeruginosa* virulence genes. *Proc. Natl. Acad. Sci. U.S.A.* 91, 197–201. doi: 10.1073/pnas.91.1.197
- Pearson, J. P., Passador, L., Iglewski, B. H., and Greenberg, E. P. (1995). A second N-acylhomoserine lactone signal produced by *Pseudomonas aeruginosa*. *Proc. Natl. Acad. Sci. U.S.A.* 92, 1490–1494. doi: 10.1073/pnas.92.5.1490
- Penesyan, A., Gillings, M., and Paulsen, I. T. (2015). Antibiotic discovery: combatting bacterial resistance in cells and in biofilm communities. *Molecules* 20, 5286–5298. doi: 10.3390/molecules20045286
- Petronilli, V., Penzo, D., Scorrano, L., Bernardi, P., and Di Lisa, F. (2001). The mitochondrial permeability transition, release of cytochrome *c* and cell death correlation with the duration of pore openings *in situ*. *J. Biol. Chem.* 276, 12030–12034. doi: 10.1074/jbc.m010604200
- Preston, M. J., Seed, P. C., Toder, D. S., Iglewski, B. H., Ohman, D. E., Gustin, J. K., et al. (1997). Contribution of proteases and LasR to the virulence of *Pseudomonas aeruginosa* during corneal infections. *Infect. Immun.* 65, 3086–3090. doi: 10.1128/iai.65.8.3086-3090.1997
- Rasamiravaka, T., and El Jaziri, M. (2016). Quorum-sensing mechanisms and bacterial response to antibiotics in *P. aeruginosa*. *Curr. Microbiol.* 73, 747–753. doi: 10.1007/s00284-016-1101-1
- Rasmussen, T. B., and Givskov, M. (2006). Quorum-sensing inhibitors as anti-pathogenic drugs. *Int. J. Med. Microbiol.* 296, 149–161. doi: 10.1016/j.ijmm.2006.02.005
- Rasmussen, T. B., Skindersoe, M. E., Bjarnsholt, T., Phipps, R. K., Christensen, K. B., Jensen, P. O., et al. (2005). Identity and effects of quorum-sensing inhibitors produced by *Penicillium* species. *Microbiology* 151, 1325–1340. doi: 10.1099/mic.0.27715-0
- Riccardi, C., and Nicoletti, I. (2006). Analysis of apoptosis by propidium iodide staining and flow cytometry. *Nat. Protoc.* 1, 1458–1461. doi: 10.1038/nprot.2006.238
- Ritchie, A. J., Whittall, C., Lazenby, J. J., Chhabra, S. R., Pritchard, D. I., and Cooley, M. A. (2007). The immunomodulatory *Pseudomonas aeruginosa* signalling molecule N-(3-oxododecanoyl)-L-homoserine lactone enters mammalian cells in an unregulated fashion. *Immunol. Cell. Biol.* 85, 596–602. doi: 10.1038/sj.icb.7100090
- Rutherford, S. T., and Bassler, B. L. (2012). Bacterial quorum sensing: its role in virulence and possibilities for its control. *Cold Spring Harb. Perspect. Med.* 2:a012427. doi: 10.1101/cshperspect.a012427
- Sadikot, R. T., Blackwell, T. S., Christman, J. W., and Prince, A. S. (2005). Pathogen-host interactions in *Pseudomonas aeruginosa* pneumonia. *Am. J. Respir. Crit. Care Med.* 171, 1209–1223.
- Santajit, S., Seesuy, W., Mahasongkram, K., Sookrung, N., Ampawong, S., Reamtong, O., et al. (2019). Human single-chain antibodies that neutralize *Pseudomonas aeruginosa*-exotoxin A-mediated cellular apoptosis. *Sci. Rep.* 9, 1–15.
- Sarabhai, S., Sharma, P., and Capalash, N. (2013). Ellagic acid derivatives from *Terminalia chebula* Retz. downregulate the expression of quorum sensing genes to attenuate *Pseudomonas aeruginosa* PAO1 virulence. *PLoS One* 8:e53441. doi: 10.1371/journal.pone.0053441
- Schwarzer, C., Fu, Z., Patanwala, M., Hum, L., Lopez-Guzman, M., Illek, B., et al. (2012). *Pseudomonas aeruginosa* biofilm-associated homoserine lactone C12 rapidly activates apoptosis in airway epithelia. *Cell. Microbiol.* 14, 698–709. doi: 10.1111/j.1462-5822.2012.01753.x
- Shiner, E. K., Terentyev, D., Bryan, A., Sennoune, S., Martinez-Zaguilan, R., Li, G., et al. (2006). *Pseudomonas aeruginosa* autoinducer modulates host cell responses through calcium signalling. *Cell. Microbiol.* 8, 1601–1610. doi: 10.1111/j.1462-5822.2006.00734.x
- Shreaz, S., Wani, W. A., Behbehani, J. M., Raja, V., Irshad, M., Karched, M., et al. (2016). Cinnamaldehyde and its derivatives, a novel class of antifungal agents. *Fitoterapia* 112, 116–131. doi: 10.1016/j.fitote.2016.05.016
- Silva Filho, L. V. R. F., Ferreira, F. D. A., Reis, F. J. C., Britto, M. C. A. D., Levy, C. E., Clark, O., et al. (2013). *Pseudomonas aeruginosa* infection in patients with cystic fibrosis: scientific evidence regarding clinical impact, diagnosis, and treatment. *J. Bras. Pneumol.* 39, 495–512. doi: 10.1590/s1806-37132013000400015
- Smith, G. P. (1985). Filamentous fusion phage: novel expression vectors that display cloned antigens on the virion surface. *Science* 228, 1315–1317. doi: 10.1126/science.4001944
- Smith, R. S., Harris, S. G., Phipps, R., and Iglewski, B. (2002). The *Pseudomonas aeruginosa* quorum-sensing molecule N-(3-oxododecanoyl) homoserine lactone contributes to virulence and induces inflammation *in vivo*. *J. Bacteriol.* 184, 1132–1139. doi: 10.1128/jb.184.4.1132-1139.2002
- Soto-Aceves, M. P., Cocotl-Yañez, M., Merino, E., Castillo-Juárez, I., Cortés-López, H., González-Pedraja, B., et al. (2019). Inactivation of the quorum-sensing transcriptional regulators LasR or RhlR does not suppress the expression of virulence factors and the virulence of *Pseudomonas aeruginosa* PAO1. *Microbiology* 165, 425–432. doi: 10.1099/mic.0.000778
- Sultan, A., and Sokolove, P. M. (2001). Free fatty acid effects on mitochondrial permeability: an overview. *Arch. Biochem. Biophys.* 386, 52–61. doi: 10.1006/abbi.2000.2195
- Tang, H. B., DiMango, E., Bryan, R., Gambello, M., Iglewski, B. H., Goldberg, J. B., et al. (1996). Contribution of specific *Pseudomonas aeruginosa* virulence factors to pathogenesis of pneumonia in a neonatal mouse model of infection. *Infect. Immun.* 64, 37–43. doi: 10.1128/iai.64.1.37-43.1996
- Tao, S., Luo, Y., He, B., Liu, J., Qian, X., Ni, Y., et al. (2016). Paraoxonase 2 modulates a proapoptotic function in LS174T cells in response to quorum sensing molecule N-(3-oxododecanoyl)-L-homoserine lactone. *Sci. Rep.* 6:28778.
- Tao, S., Niu, L., Cai, L., Geng, Y., Hua, C., Ni, Y., et al. (2018). N-(3-oxododecanoyl)-L-homoserine lactone modulates mitochondrial function and suppresses proliferation in intestinal goblet cells. *Life Sci.* 201, 81–88. doi: 10.1016/j.lfs.2018.03.049
- Tapryal, S., Gaur, V., Kaur, K. J., and Salunke, D. M. (2013). Structural evaluation of a mimicry-recognizing paratope: plasticity in antigen-antibody interactions manifests in molecular mimicry. *J. Immunol.* 191, 456–463. doi: 10.4049/jimmunol.1203260
- Tateda, K., Ishii, Y., Horikawa, M., Matsumoto, T., Miyairi, S., Pechere, J. C., et al. (2003). The *Pseudomonas aeruginosa* autoinducer N-3-oxododecanoyl homoserine lactone accelerates apoptosis in macrophages and neutrophils. *Infect. Immun.* 71, 5785–5793. doi: 10.1128/iai.71.10.5785-5793.2003
- Trott, O., and Olson, A. J. (2010). AutoDock Vina: improving the speed and accuracy of docking with a new scoring function, efficient optimization, and multithreading. *J. Comput. Chem.* 31, 455–461.
- Venturi, V. (2006). Regulation of quorum sensing in *Pseudomonas*. *FEMS Microbiol. Rev.* 30, 274–291.
- Wagner, V. E., Bushnell, D., Passador, L., Brooks, A. I., and Iglewski, B. H. (2003). Microarray analysis of *Pseudomonas aeruginosa* quorum-sensing regulons: effects of growth phase and environment. *J. Bacteriol.* 185, 2080–2095. doi: 10.1128/jb.185.7.2080-2095.2003
- Waters, C. M., and Goldberg, J. B. (2019). *Pseudomonas aeruginosa* in cystic fibrosis: a chronic cheater. *Proc. Natl. Acad. Sci. U.S.A.* 116, 6525–6527.
- Wing, M. G. (1995). The molecular basis for a polyspecific antibody. *Clin. Exp. Immunol.* 99, 313–315. doi: 10.1111/j.1365-2249.1995.tb05551.x
- Wyllie, A. H., Kerr, J. R., and Currie, A. R. (1980). Cell death: the significance of apoptosis. *Int. Rev. Cytol.* 68, 251–306. doi: 10.1016/s0074-7696(08)62312-8
- Xu, D., and Zhang, Y. (2011). Improving the physical realism and structural accuracy of protein models by a two-step atomic-level energy minimization. *Biophys. J.* 101, 2525–2534. doi: 10.1016/j.bpj.2011.10.024
- Yang, J., Yan, R., Roy, A., Xu, D., Poisson, J., and Zhang, Y. (2015). The I-TASSER suite: protein structure and function prediction. *Nat. Methods* 12, 7–8. doi: 10.1038/nmeth.3213
- Zhang, J. H., and Ming, X. U. (2000). DNA fragmentation in apoptosis. *Cell Res.* 10, 205–211.

**Conflict of Interest:** The authors declare that the research was conducted in the absence of any commercial or financial relationships that could be construed as a potential conflict of interest.

Copyright © 2020 Santajit, Seesuy, Mahasongkram, Sookrung, Pumirat, Ampawong, Reamtong, Chongsa-Nguan, Chaicumpa and Indrawattana. This is an open-access article distributed under the terms of the Creative Commons Attribution License (CC BY). The use, distribution or reproduction in other forums is permitted, provided the original author(s) and the copyright owner(s) are credited and that the original publication in this journal is cited, in accordance with accepted academic practice. No use, distribution or reproduction is permitted which does not comply with these terms.